AN OVERVIEW OF LTE-ADVANCED PRO'S FULL-DIMENSION MIMO

Dr. Yogesh Bhomia, Dr. Sunil Kumar Mishra, Mr. R K Tiwari
[1,3] ECE Dept,[2] CSE Dept, Accurate Institute Of Management & Technology, Greater Noida

Abstract
In order to reduce the processing complexity, energy consumption, and spectrum efficiency of next-generation cellular systems, multiple-input multiple-output (MIMO) systems with a large number of base station antennas—also referred to as massive MIMO—have drawn a lot of attention from both academia and industry. With the need for future wireless systems growing, the mobile communication industry has started a feasibility study of huge MIMO systems. In the third generation partnership project (3GPP), the Full-Dimension MIMO (FD-MIMO), an official name for the MIMO improvement, has shown potential benefits in field trials of proof-of-concept systems. To ensure this technology's smooth integration into the current 4G LTE systems, 3GPP started standardisation efforts. We present a summary of the FD-MIMO technology in this post, focusing on the conversation and controversy surrounding Release 13's standardisation process. We provide performance evaluations for common FD-MIMO scenarios, an overview of the main concerns for standardisation and feasible system design, and important features for FD-MIMO systems.

I. INTRODUCTION

Multiple-input multiple-output (MIMO) systems with a large number of basestation antennas, often referred to as massive MIMO systems, have received much attention in academia and indus- try as a means to improve the spectral efficiency, energy efficiency, and processing complexity [1]. While the massive MIMO technology is a promising technology, there are many practical chal- lenges and technical hurdles down the road to the successful commercialization. These include design of low-cost and low-power basestation with acceptable antenna space, improvement in the fronthaul capacity between radio and control units, acquisition of high dimensional channel state information (CSI), and many others. Recently, 3rd generation partnership project (3GPP) standard body initiated the standardization activity to employ tens of antennas at basestation with an aim to satisfy the spectral efficiency requirement of future cellular systems [2], [3]. Considering the implementation cost and complexity, and also the timeline to the real deployment, 3GPP decided to use tens of antennas with a two dimensional (2D) array structure as a starting point. Full-Dimension MIMO (FD-MIMO), the official name for the MIMO enhancement in 3GPP, targets the system utilizing up to 64 antenna ports at the transmitter side. Recently, field trials of the proof-of-concept FD-MIMO systems have been conducted successfully [4]. A study item, a process done before a formal standardization process, has been completed in June 2015, and the follow-up work item process will be finalized soon for the formal standardization of Release 13 (Rel. 13).1

The purpose of this article is to provide an overview of the FD-MIMO systems with an emphasis on the discussion and debate conducted on the standardization process of Rel. 13. We note that preliminary studies addressed the feasibility of 2D array antenna structure and

performance evaluation in ideal pilot transmission and feedback scenarios [2], [3]. This work is distinct from these in the sense that we put our emphasis on describing realistic issues in the standardization process, including TXRU architectures, beamformed CSI-RS, 3D beamforming, details of CSI feedback, and performance evaluation in realistic FD-MIMO scenarios with new feedback schemes.

II. KEY FEATURES OF FD-MIMO SYSTEMS

In this section, we discuss key features of FD-MIMO systems. These include a large number of basestation antennas, 2D active antenna array, 3D channel propagation, and new pilot transmission with CSI feedback. In what follows, we will use LTE terminology exclusively: enhanced node-B (eNB) for basestation, user equipment (UE) for the mobile terminal, and reference signal (RS) for pilot signal.

A. Increase the number of transmit antennas

One of the main features of FD-MIMO systems distinct from the MIMO systems of the current LTE and LTE-Advanced standards is to use a large number of antennas at eNB. In theory, as the number of eNB antennas NT increases, cross-correlation of two random channel realizations goes to zero [1] so that the inter-user interference in the downlink can be controlled via a simple linear precoder. Such benefit, however, can be realized only when the perfect CSI is available at the eNB. While the CSI acquisition in time division duplex (TDD) systems is relatively simple due to the channel reciprocity, such is not the case for frequency division duplex (FDD) systems. Note that in the FDD systems, time variation and frequency response of the channel are measured via the downlink RSs and then sent back to the eNB after the quantization. Even in TDD mode, one cannot solely rely on the channel reciprocity because the measurement at the transmitter does not capture the downlink interference from neighboring cells or co-scheduled UEs. As such, downlink RSs are still required to capture the channel quality indicator (CQI) for the TDD mode, and thus the downlink RS and the uplink CSI feedback are essential for both duplex modes. Identifying the potential issues of CSI acquisition and developing the proper solutions are, therefore, of great importance for the successful commercialization of FD-MIMO systems. Before we go into detail, we briefly summarize two major problems related to the CSI acquisition.

• Degradation of CSI accuracy: One well-known problem for the MIMO systems, in particular for FDD-based systems, is that the quality of CSI is affected by the limitation of feedback resources. As the CSI distortion increases, quality of the multiuser MIMO (MU-MIMO) precoder to control the inter-user interference is degraded and so will be the performance of the FD-MIMO systems. In general, the amount of CSI feedback, determining the quality of CSI, needs to be scaled with NT to control the quantization error so that the overhead of CSI feedback increases in FD-MIMO systems.

• Increase of pilot overhead: An important problem related to the CSI acquisition at eNB, yet to be discussed separately, is the pilot overhead problem. UE performs the channel estimation using the RS transmitted from the eNB. Since RSs need to be assigned in an orthogonal fashion, RS overhead typically grows linearly with NT . For example, if NT = 64, RS will occupy approximately 48% of resources, eating out substantial amount of downlink resources for the data transmission.

B.   2D active antenna system (AAS)

Another interesting feature of the FD-MIMO system is an introduction of the active antenna with 2D planar array. In the active antenna-based systems, gain and phase are controlled by the active components, such as power amplifier (PA) and low noise amplifier (LNA), attached to each antenna element. In the 2D structured antenna array, one can control the radio wave on both vertical (elevation) and horizontal (azimuth) direction so that the control of the transmit beam in 3D space is possible. This type of wave control mechanism is also referred to as the 3D beamforming. Another important benefit of 2D AAS is that it can accommodate a large number of antennas without increasing the deployment space. For example, when 64 linear antenna arrays are deployed in a horizontal direction, under the common assumption that the antenna spacing is half wavelength (λ) and the system is using LTE carrier frequency (2 GHz), it requires a horizontal room of 3m. Due to the limited space on a rooftop or mast, this space would be burdensome for most of the cell sites. In contrast, when antennas are arranged in a square array, relatively small space is required for 2D antenna array (e.g., 1.0×0.5m with dual-polarized 8

$\times$ 8 antenna array).

C.   3D channel environment

When basic features of the FD-MIMO systems are determined, the next step is to design a system maximizing performance in terms of throughput, spectral efficiency, and peak data rate in the realistic channel environment. There are various issues to consider in the design of practical systems, such as investigation and characterization of the realistic channel model for the performance evaluation. While the conventional MIMO systems consider the propagation in the horizontal direction only, FD-MIMO systems employing 2D planar array should consider the propagation in both vertical and horizontal direction. To do so, geometric structure of the transmitter antenna array and propagation effect of the 3D positions between the eNB and UE should be reflected in the channel model. Main features of 3D channel propagation obtained from real measurement are as follows [5]:

•   Height and distance-dependent line-of-sight (LOS) channel condition: LOS probability be- tween eNB and UE increases with the UE's height and also increases when the distance between eNB and UE decreases.

•   Height-dependent pathloss: UE experiences less pathloss on a higher floor (e.g., 0.6dB/m gain for macro cell and 0.3dB/m gain for micro cell).

•   Height and distance-dependent elevation spread of departure angles (ESD): When the lo- cation of eNB is higher than the UE, ESD decreases with the height of the UE. It is also observed that the ESD decreases sharply as the UE moves away from the eNB.

D.   RS transmission for CSI acquisition

From the LTE to LTE-Advanced, there has been substantial improvement in the RS scheme for MIMO systems (see Fig. 1(a)). From the common RS (CRS) to the channel state information RS (CSI-RS), various RSs to perform the CSI acquisition have been introduced. While these are common to all users in a cell and thus un-precoded, the demodulation RS (DM-RS) is UE- specific (i.e., dedicated to each UE) so that it is precoded by the same weight applied

for the data transmission. Since the DM-RS is present only on time/frequency resources where the UE is scheduled, this cannot be used for CSI measurements [6].

One of the new features of the FD-MIMO systems is to use a beamformed RS, called beamformed CSI-RS, for the CSI acquisition. Beamformed RS transmission is a channel training technique that uses multiple precoding weights in spatial domain. In this scheme, UE picks the best weight among transmitted and then feeds back its index. This scheme provides many benefits over non-precoded CSI-RS, in particular when NT is large. Some of the benefits are summarized as follows:
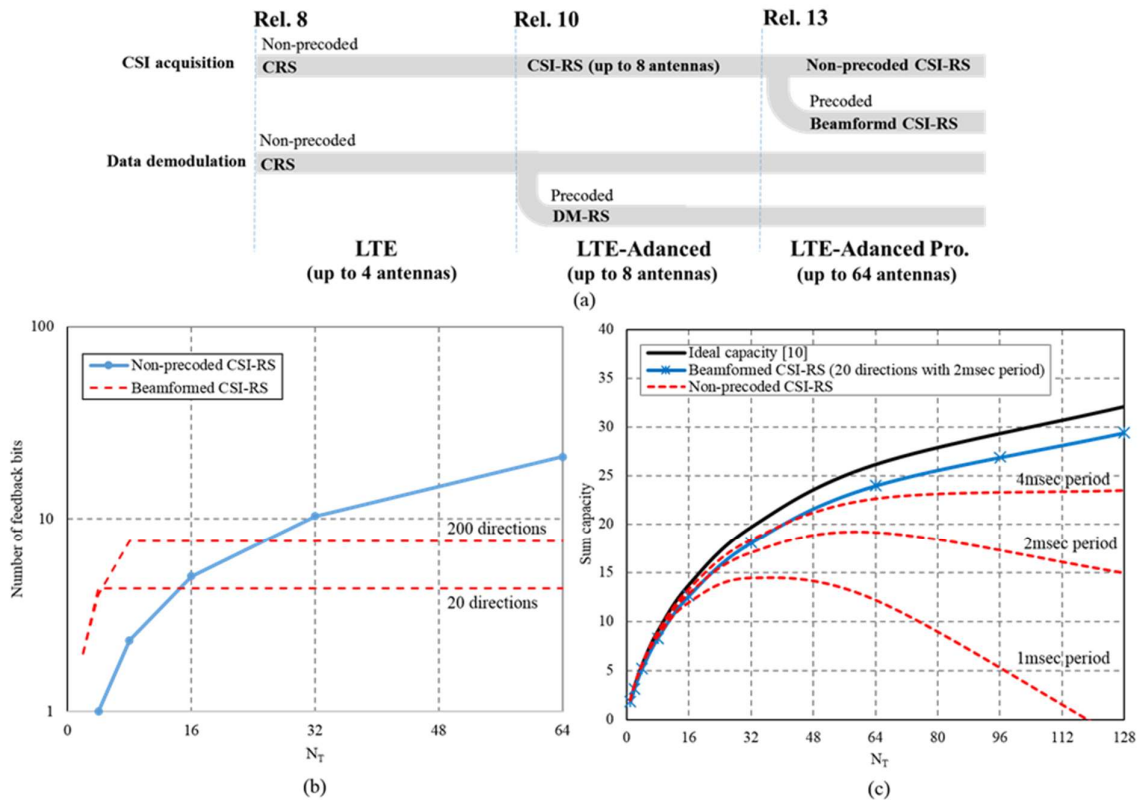
Fig. 1. MIMO evaluation: (a) RS evolution in LTE systems, (b) uplink feedback overhead (SNR=10dB [7]), (c) MU-MIMO capacity with considering CSI-RS overhead (ideal CSI and ZFBF MU-precoding with 10 UEs and SNR=10dB).

• Less uplink feedback overhead: In order to maintain a rate comparable to the case with perfect CSI, feedback bits used for the channel vector quantization should be proportional to NT [7]. Whereas, the amount of feedback for the beamformed CSI-RS scales logarithmic with the number of RSs NB since this scheme only feeds back an index of the best beamformed CSI-RS. Thus, as depicted in Fig. 1(b), the benefit of beamformed CSI-RS is pronounced when NT is large.

• Less downlink pilot overhead: When the non-precoded CSI-RS is used, pilot overhead increases with NT , resulting in a substantial loss of the sum capacity in the FD-MIMO regime (see Fig. 1(c)). Whereas, pilot overhead of the beamformed CSI-RS is proportional to NB and independent of NT so that the rate loss of the beamformed CSI-RS is marginal even when NT increases.

- Higher quality in RS: If the transmit power is P watt, P/NT watt is needed for each non-precoded CSI-RS transmission, while P/NB watt is used for the beamformed CSI-RS. For example, when NT = 32 and NB = 12, beamformed CSI-RS provides 4.3dB gain in signal power over the non-precoded CSI-RS.2

In order to support the beamformed CSI-RS scheme, new transmitter architecture called transceiver unit (TXRU) architecture has been introduced. By TXRU architecture, we mean a hardware connection between the baseband signal path and antenna array elements. Since this architecture facilitates the control of phase and gain in both digital and analog domain, more accurate control of the beamforming direction is possible. One thing to note is that the conventional codebook cannot measure the CSI of the beamformed transmission so that a new channel feedback mechanism supporting the beamformed transmission is required (see Section III.D for details).

III.   SYSTEM DESIGN AND STANDARDIZATION OF FD-MIMO SYSTEMS

The main purpose of the Rel. 13 study item is to identify key issues to support up to 64 transmit antennas placed in the form of a 2D antenna array. Standardization of the systems supporting up to 16 antennas is an initial target of Rel. 13 and issues to support more than 16 antennas will be discussed in subsequent releases. In the study item phase, there has been extensive discussion to support 2D array antennas, elaborated TXRUs, enhanced channel measurement and feedback schemes, and also an increased number of co-scheduled users (up to eight users). Among these, an item tightly coupled to the standardization is the CSI measurement and feedback mechanism. In this subsection, we discuss the deployment scenarios, antenna configurations, TXRU structure, new RS strategy, and feedback mechanisms.

A.   Deployment scenarios

For the design and evaluation of FD-MIMO systems, a realistic scenario in which antenna array and UEs are located in different height is considered. To this end, two typical deployment scenarios, viz., 3D urban macro scenario (3D-UMa) and 3D urban micro (3D-UMi), are introduced (see Fig. 2). In the former case, transmit antennas are placed over the rooftop, and in the latter case, they are located below the rooftop. In case of 3D-UMa, diffraction over the rooftop is a dominant factor for the propagation so that down-tilted transmission in the vertical direction is desirable (see Fig. 2(b)). In fact, by transmitting beams with different steering angles, eNB can separate channels corresponding to multiple UEs. In the 3D-UMi scenario, on the other hand, the location of users is higher than the height of the antenna so that direct signal path is dominant (see Fig. 2(c)). In this scenario, both up and down-tilting can be used to schedule UEs in different floors. Since the cell radius of the 3D-UMi scenario is typically smaller than that of 3D-UMa, LOS channel condition is predominant, and thus more UEs can be co-scheduled without increasing the inter-user interference [5]. Although not as strong as the 3D-UMi scenario, LOS probability in the 3D-UMa scenario also increases when the distance between eNB and UE decreases.

B.   Antenna configurations

Unlike the conventional MIMO systems relying on the passive antenna, systems based on the active antenna can dynamically control the gain of an antenna element by applying the weight of low-power amplifiers attached to each antenna element. Since the radiation pattern depends on the antenna arrangement, such as the number of the antenna elements and antenna spacing, the antenna system should be modeled in an element-level. As shown in Fig. 3(a), there are three key parameters characterizing the antenna array structure (M, N, P): the number of elements M in vertical direction, the number of elements N in horizontal direction, and the polarization degree P (P = 1 is for co-polarization and P = 2 is for dual-polarization). As a benchmark setting, 2D planar array using dual polarized antenna (P = 2) configuration with M = 8 (0.8λ spacing in vertical direction) and N = 4 (0.5λ spacing in horizontal direction) is suggested.3 In this setting, null direction, an angle to make the magnitude of beam pattern to zero, for the elevation beam pattern is 11◦ and that for the horizontal beam pattern is 30◦ (see Fig. 3(c)). Since the null direction in the vertical domain is much smaller than that of the horizontal domain, scheduling UEs in the vertical domain is more effective in controlling the inter-user interference. Also, a tall or fat array structure (M N or M N) is favorable since it will generate a
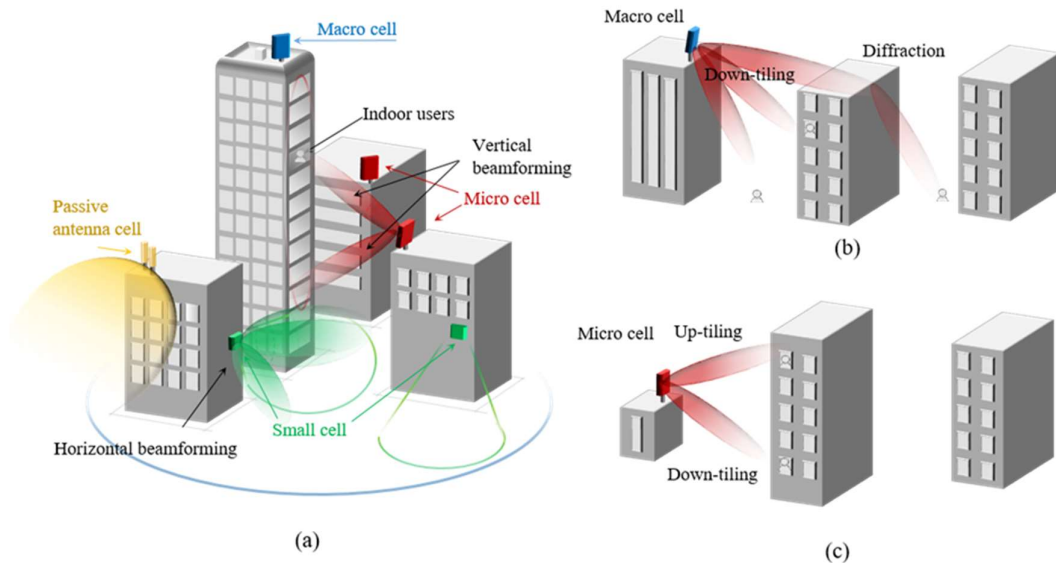

Fig. 2. FD-MIMO deployment scenarios: (a) 3D macro cell site (placed over the rooftop) and 3D micro cell site (placed below the rooftop) with small cell, (b) beamforming for 3D macro cell, and (c) beamforming in 3D micro cell.

sharp beam but it might be less flexible in the situation where the surrounding environment is changed. Further, large antenna spacing is not always a desirable option since it can increase the inter-cell interference due to the narrow beamforming for cell edge UEs (this phenomenon is called flash-light effect). For this reason, in a real deployment scenario, the design parameters should be carefully chosen by considering various factors, such as user location, cell radius, building height, and antenna height.

C.   TXRU architectures

As mentioned, one interesting feature of the active antenna systems is that each TXRU contains PA and LNA so that eNB can control the gain and phase of an individual antenna element. In order to support this, a power feeding network between TXRUs and antenna elements called TXRU architecture is introduced [9]. TXRU architecture consists of three components: TXRU array, antenna array, and radio distribution networks (RDN). A role of the RDN is to deliver the transmit signal from PA to antenna array elements and the received signal from antenna array to LNA. Depending on the CSI-RS transmission and feedback strategy, two representative
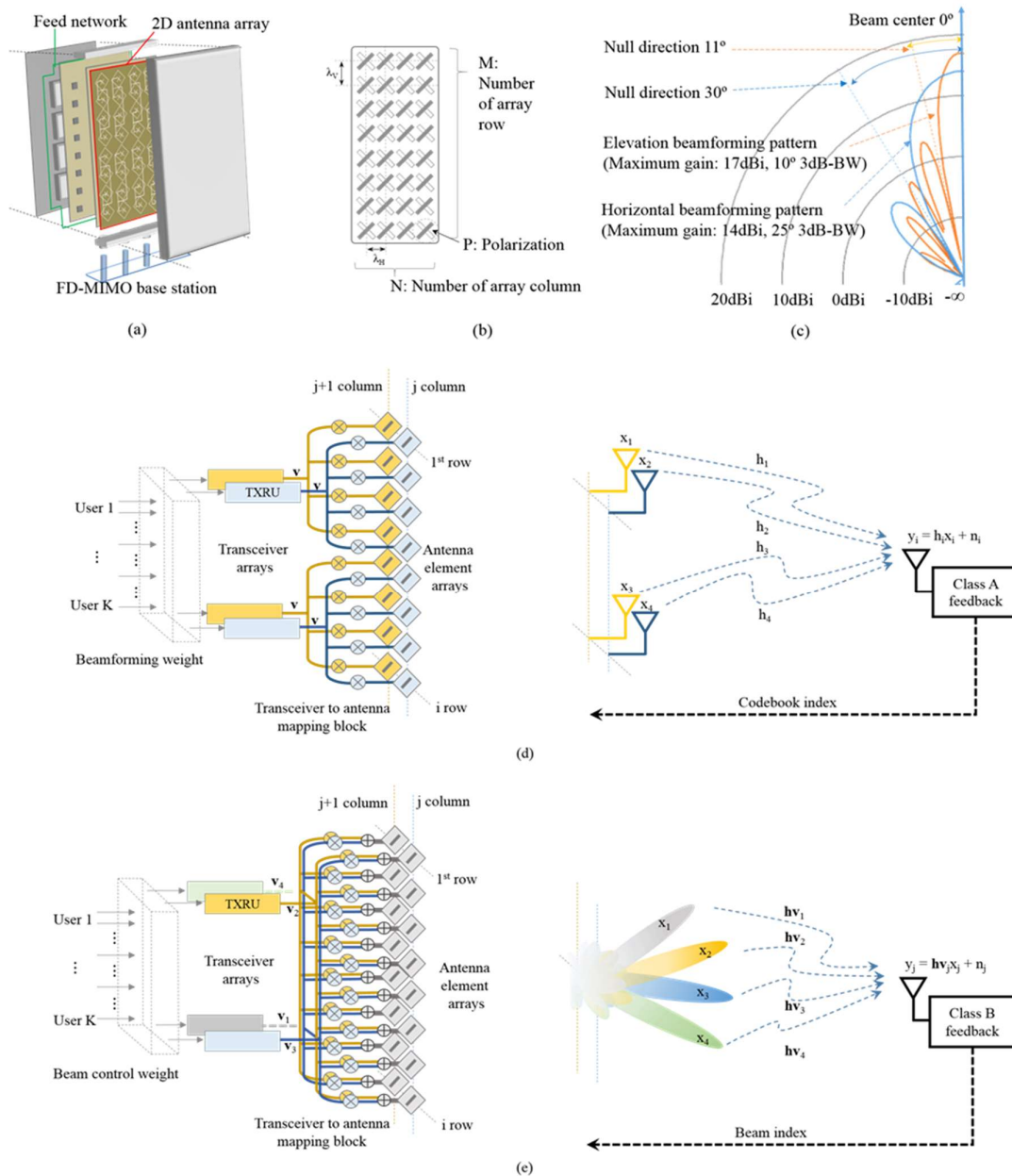

Fig. 3. FD-MIMO systems: (a) concept of FD-MIMO systems, (b) 2D array antenna configuration, (c) vertical and horizontal beamforming patterns, (d) array partitioning architecture with the conventional CSI-RS transmission, and (e) array connected architecture with beamformed CSI-RS transmission.

options, array partitioning and array connected architecture, are suggested. The former is for the conventional codebook scheme and the latter is for the beamforming scheme.

In the array partitioning architecture, antenna elements are divided into multiple groups and each TXRU is connected to one of them (see Fig. 3(d)). Whereas, in the array connected structure, RDN is designed such that RF signals of multiple TXRUs are delivered to the single antenna element. To mix RF signals from multiple TXRUs, additional RF combining circuitry is needed as shown in Fig. 3(e). The difference between the two can be better understood when we discuss the transmission of the CSI-RS. In the array partitioning architecture, NT antenna elements are partitioned into L groups of TXRU and orthogonal CSI-RS is assigned for each group. Each TXRU transmits its own CSI-RS so that the UE measures the channel h from the CSI-RS observation y = hx + n. In the array connected architecture, each antenna element is connected

to L' (out of L) TXRUs and orthogonal CSI-RS is assigned for each TXRU. Denoting h $\in$ C1×Nc as the channel vector and v $\in$ CNc×1 as the precoding weight (NT L = Nc) for each beamformed

CSI-RS, the beamformed CSI-RS observation is y = hvx+n and the UE measures the precoded channel hv from this. Due to the narrow and directional CSI-RS beam transmission with a linear array, SNR of the precoded channel is maximized at the target direction.[4]

D. New CSI-RS transmission strategy

In the standardization process, two CSI-RS transmission strategies, i.e., extension of the conventional non-precoded CSI-RS and the beamformed CSI-RS, are suggested. In the first strategy, UE observes the non-precoded CSI-RS transmitted from each of partitioned antenna arrays (see Fig.3(d)). By sending the precoder maximizing the properly designed performance criterion to the eNB, UE can adapt to the channel variation. In the second strategy, eNB transmits multiple beamformed CSI-RS (we call it beam for simplicity) using connected arrays architecture. Among these, UE selects the preferred beam and then feeds back its index. When the eNB receives the beam index, the weight corresponding to the selected beam is used for the data transmission.

Overall downlink precoder for data transmission Wdata and CSI-RS transmission Wrs can be expressed as

$$Wdata = WT\ Wrs\quad and\quad Wrs = WP\ WU\ ,\qquad (1)$$

where WT $\in$ CNT ×L is the precoder between TXRU and the antenna element, WP $\in$ CL×NP is the precoder between the CSI-RS port and the TXRU (NP is the number of antenna ports), and WU $\in$ CNP ×r is the precoder between data channel to CSI-RS port.

In the following, we summarize details of two strategies.

• Conventional CSI-RS transmission: One option to maximize the capacity is to do one-to- one mapping of the TXRU and the CSI-RS resource (i.e., WP = INTXRU). To achieve the same coverage for each CSI-RS resource, an identical weight v is applied to L groups.[5] Each UE measures the CSI-RS resources and then chooses the preferred codebook index i∗ maximizing the channel gain for each subband:

i∗ = arg max

i

$\bar{h}^H W_i$

2,   (2)

where $\bar{a}^2 = q\Sigma |a_i|^2$ and $\bar{h} = h/\|h\|^2$ is the estimated channel direction vector, and i is the ith precoder between the data channel and CSI-RS ports. This scheme is called class-A CSI feedback.

• Beamformed CSI-RS transmission: In order to acquire the spatial angle between the eNB and UE, eNB transmits multiple beamformed CSI-RSs. Let NB be the number of CSI-RSs, then we have WT = [v1v2 . . . vN] where vi ∈ CNT ×1 is the 3D beamforming weight for the ith beam. For example, when the rank-1 beamforming is applied, we have WP = 1NB and WU = 1. Among all possible beams v1, ..., vNB , UE selects and feeds back the best beam index j∗ maximizing the received power:

j∗ = arg max|$\bar{h}^H$ vj|2.(3)
j

This scheme is called class-B CSI feedback. Under the rich scattering environment, dom- inant paths between eNB and UE depend on the direction and width of the transmit signal. In the multiple-input single-output (MISO) channel, for example, the channel vector

in an angular domain is expressed as h = Σi

$e_r e_t(\varphi_i)^*$, where $e_r = 1$ and $e_t(\varphi_i) =$

5In this paper, we assume that discrete Fourier transform (DFT) weights are used as WT for mapping between TXRU and antenna elements for simplicity. For example, WT can be expressed as WT = [v v; v v] in Fig. 3(d).

TABLE I
COMPARISON BETWEEN CSI-RS TRANSMISSION AND CSI FEEDBACK CLASSES

Category	Class-A CSI feedback (Conventional CSI-RS)	Class-B CSI feedback (Beamformed CSI-RS)
Feedback design	Need to design codebook for 2D antenna layout and feedback mechanism for adapting channel variation	Need to devise a method to feed back beam index for adapting both weight changes and channel variation
UL Feedback overhead	Depend on resolution of codebook and the number of antennas	Depend on the number of operating beam N_B
CSI-RS overhead	Require N_T CSI-RS resources	Scale linearly with the number of beam N_B
Backward compatibility	Supportable with virtualization between TXRUs and antenna ports	Supportable with vertical 1D beamforming weight

Forward compatibility	Scalable to larger TXRU system if CSI-RS resources are allowed	Scalable to larger TXRU system if long-term channel statistics are acquired

$[1 \ e^{-j2\pi\gamma\varphi i} \ ... \ e^{-j2\pi(NT-1)\gamma\varphi i}]T$ is the spatial signature of the transmitter (φi is direction of ith path and γ is normalized antenna spacing) [10]. When the RS is transmitted in a direction φj, the beamforming weight would be $v = et(\varphi j)$ so that the resulting beamformed channel is readily expressed as one or at most a few dominant taps ($et(\varphi i)T \ et(\varphi i) \approx 0$ when i /= j). In fact, by controlling the weight applied to CSI-RS, the effective dimension of the channel vector can be reduced so that the feedback overhead can be reduced substantially.

In Table I, we summarize two CSI-RS transmission schemes discussed in the FD-MIMO.

E.   CSI feedback mechanisms for FD-MIMO systems

In the study item phase, various RS transmission and feedback schemes have been proposed. As shown in Fig. 1, capacity and overhead of class-A and class-B feedback schemes are more or less similar in the initial target range (Nt = 16) so that Rel. 13 has decided to support both classes. In this subsection, we briefly describe the CSI feedback schemes associated with TXRU architectures. Among various schemes, composite codebook and beam index feedback have received much attention as main ingredients for class-A and class-B CSI feedback. The rest will be considered in a future release.

Composite codebook: In this scheme, overall codebook is divided into two (vertical and horizontal codebooks) and thus the channel information is separately delivered to the eNB. By combining two codebooks (e.g., Kronecker product of two codebooks WU = WU,V ⊗ WU,H), eNB reconstructs whole channel information. Considering that the angular spread of the vertical direction is smaller than that of the horizontal direction, one can reduce the feedback overhead by setting a relatively long reporting period to the vertical codebook.

Beam index feedback: To obtain the UE's channel direction information (CDI) from beam-formed CSI-RSs, eNB needs to transmit multiple beamformed CSI-RSs. When the channel rank is one, feedback of a beam index and corresponding CQI is enough. Whereas, when the channel rank is two with dual-polarized antennas, co-phase information is additionally required for adapting channel orthogonalization between layers. For example, once eNB obtains the CDI, this can be used for the beamforming vector of two-port CSI-RS and each CSI-RS port is mapped to the different polarized antennas. UE then estimates and feeds back short-term co-phase information between two ports.

Other CSI feedback schemes: In the partial CSI-RS transmission, CSI-RS overhead can be reduced by partitioning the 2D antenna array into horizontal and vertical ports, say NH ports in the row and NV ports in the column. In doing so, the total number of CSI-RS can be reduced from

NH × NV to NH + NV . Overall channel information can be reconstructed by exploiting spatial and temporal correlation among antenna elements [11]. In the adaptive CSI feedback scheme, benefits of the beamformed and non-precoded CSI-RS transmission can be combined. First, in order to acquire long-term channel information, eNB transmits NT non-precoded CSI-RSs. After receiving sufficient long-term channel statistics from UE, eNB determines spatial direction roughly and then transmits the beamformed CSI-RSs used for short-term and subband

feedbacks. The flexible codebook scheme can support various 2D antenna layouts without increasing the number of codebooks. In this approach, one master codebook is designed for a large number
of TXRUs, say 16 TXRUs, and the specific codebook (e.g., (2×8), (4×4), or (1×16)) is derived based on this. To support this, the eNB needs to send the layout information via separate signaling.

IV.   PERFORMANCE OF FD-MIMO SYSTEM

In order to observe the potential gain of the FD-MIMO systems, we perform system-level simulations under the realistic multicell environment. In our simulations, we test two typical deployment scenarios (3D-UMa and 3D-UMi) with 2-tier hexagonal layout. As a performance metric, we use spectral efficiency for cell average and cell edge. Detailed simulation parameters are provided in Table II. We first investigate the system performance of FD-MIMO systems with two types of antenna configurations. For type I and II configurations, $(M, N, P) = (8, 4, 2)$ and $(M, N, P) = (32, 4, 2)$ are used, respectively. In the type II configuration, antenna spacing is set to four times larger than the spacing of type I. To investigate the effect of antenna structure, the ideal feedback under the full buffer traffic model (each user has an unlimited amount of data to transmit) is used. In Fig. 4(a), we plot the throughput of the conventional LTE systems with 8Tx ($NV \times NH = 1 \times 8$) and FD-MIMO systems with 16, 32, and 64Tx ($NV \times NH = 2 \times 8$, 4×8, and 8×8), where NV and NH are the number of CSI-RS in vertical and horizontal dimensions, respectively. This result shows that both antenna configurations provide a large gain over the conventional 8Tx in LTE-A, resulting in 105% (type I) and 484% (type II) gain at cell edge, respectively. Due to the sufficient antenna spacing, cross-correlation between channels becomes negligible, and thus the spectral efficiency of type II increases linearly with the TXRU, resulting in 30% (cell average) and 70% gain (cell edge) when the number of TXRUs is doubled [?]. However, due to the insufficient antenna spacing, the spectral efficiency of type I configuration does not scale linearly with the number of TXRUs.

We next investigate the system performance under the finite traffic model (e.g., FTP model) where each UE with distinct arrival time receives a file with finite size. As a performance metric, we use a user packet throughput, the number of successively received packets during the transmission period. In order to support the backward compatibility and also perform fair comparison among schemes under test, we employ the conventional MMSE-based channel estimation. In our simulations, the following CSI feedback strategies are considered.

•   Conventional 8Tx LTE Systems: Rel. 10 LTE-A feedback mechanism using 8TX codebook is used. The implicit feedback (RI, horizontal and vertical PMIs, CQI) is used for the CSI feedback.

•   **FD-MIMO systems with:**

–   Non-precoded CSI-RS: A composite codebook of horizontal and vertical codebooks is used. In case of 16Tx with ($NV \times NH = 2 \times 8$) antenna configuration, the codebook is generated via the Kronecker product of 2Tx and 8Tx LTE codebooks. The implicit feedback is used for the CSI feedback.
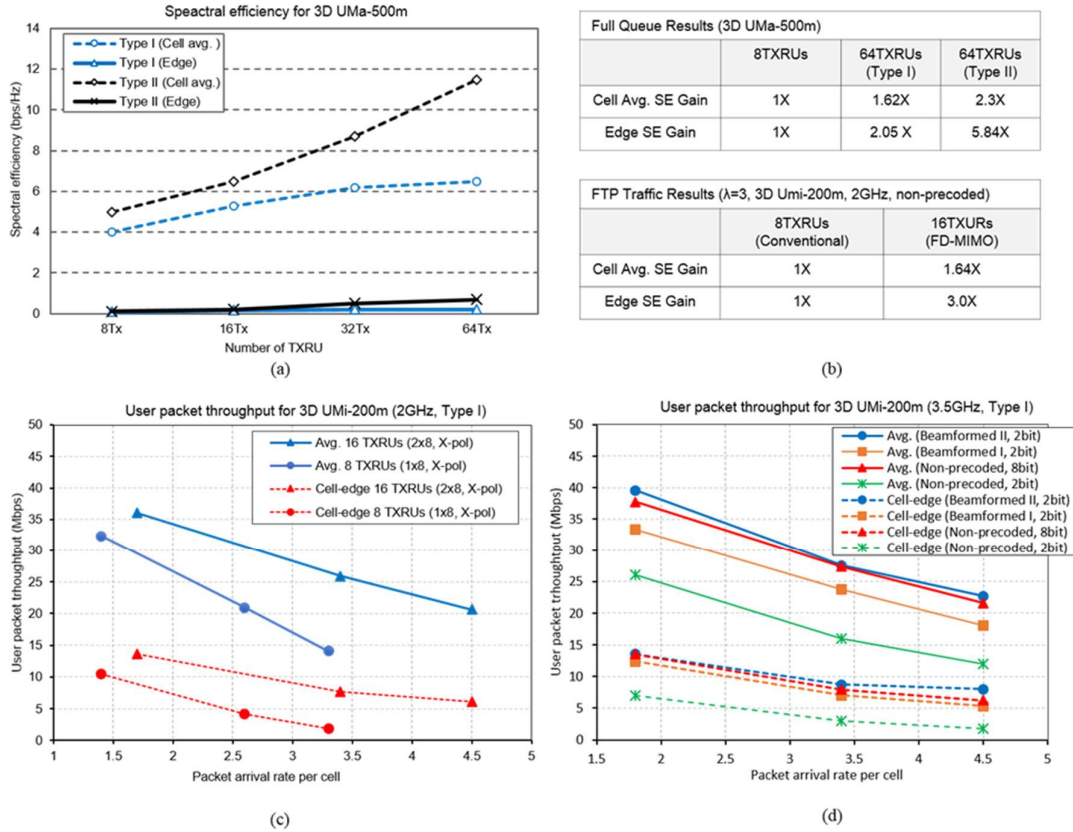
Full Queue Results (3D UMa-500m)

	8TXRUs	64TXRUs (Type I)	64TXRUs (Type II)
Cell Avg. SE Gain	1X	1.62X	2.3X
Edge SE Gain	1X	2.05 X	5.84X

FTP Traffic Results (λ=3, 3D Umi-200m, 2GHz, non-precoded)

	8TXRUs (Conventional)	16TXURs (FD-MIMO)
Cell Avg. SE Gain	1X	1.64X
Edge SE Gain	1X	3.0X

Fig. 4. System level performance results and comparison with full buffer and FTP traffic model.

– Beamformed CSI-RS scheme I: Beam index feedback is used. Four beams are used to represent the vertical angles (NB = 4). Each UE reports the best beam index (BI) and corresponding CQI.

– Beamformed CSI-RS scheme II: The eNB transmits both non-precoded and beam-formed CSI-RS. UE feeds back long-term CSI (RI, long-term PMI) using the non- precoded CSI-RSs and reports the short-term CSI (BI, CQI) using the beamformed CSI-RSs (NB = 4). The precoding weight of beamformed CSI-RS is changed based on the long-term PMI.

In Fig. 4(c), we plot the user throughput of the finite traffic model as a function of packet

arrival rate. Note that when the packet arrival rate is high, co-scheduled users need to be increased and thus the intercell and multiuser interference will also increase. In this realistic scenario, FD- MIMO systems outperform the conventional MIMO systems with a large margin, achieving

1.5× and 3× improvement in cell average and edge user packet throughput, respectively. Note that in the low network loading (low interference scenario), gain of the FD-MIMO systems is coming from the 3D beamforming. In the medium to high network loading (high interference scenario), this gain is mainly due to the multiuser precoding of the 2D active antenna array. Fig. 4(d) summarizes the throughput of various CSI feedback frameworks. With the same feedback overhead (2bit), beamformed CSI-RS scheme I outperforms the non-precoded

scheme with a large margin. This is because the number of codewords for the channel feedback is only four so that channel state information at eNB is very coarse. Since the beamformed CSI-RS scheme II can adapt weights of the beamformed CSI-RS to generate an accurate CDI, it performs best among all under tests. It is worth mentioning that the non-precoded CSI-RS scheme requires a large amount of feedback overhead (approximately 128 quantization levels) to achieve comparable performance to the CSI-RS scheme I. From this observation, we clearly see that the beamformed CSI-RS transmission is effective in controlling the precoding weights (in time, frequency, and space), feedback overhead, and pilot resource overhead.

V. CONCLUDING REMARKS

In this article, we have provided an overview of FD-MIMO systems in 3GPP LTE (recently named as LTE-Advanced Pro) with emphasis on the discussion and debate conducted on the Rel. 13 phase. We discussed key features of FD-MIMO systems and main issues in standardization of system design, such as channel model, transceiver architectures, pilot transmission, and CSI feedback scheme. To make the most of a large number of eNB antennas in a cost and space effective manner, new key features, distinct from MIMO systems in conventional LTE-A, should be introduced in the standardization, system design, and transceiver implementation. These include new transmitter architecture (array connected architecture), new RS transmission scheme (beamformed CSI-RS transmissions), and enhanced channel feedback (beam index feedback). Although our work focused primarily on the standardization in Rel. 13, there are still many issues for the successful deployment of FD-MIMO systems in the future, including pilot overhead reduction, beam adaptation and optimization, and advanced channel estimation exploiting time and angular domain sparsity [12].

TABLE II
SYSTEM SIMULATION ASSUMPTIONS

Parameter	Value
Duplex method	FDD
Bandwidth	10 MHz
Center frequency	2GHz / 3.5GHz
Inter-site distance	500m for 3D-UMa, 200m for 3D-UMi
Network synchronization	Synchronized
Cellular layout	3D Hexagonal grid, 19 eNBs, 3 cells per site
Users per cell	10 (Uniformly located in 3D space)
Downlink transmission scheme	$N_T \times 2$ MU-MIMO SLNR precoding with rank adaptation with 2 layer per UE
Downlink scheduler	Proportional Fair scheduling in the frequency and time domain.

Downlink link adaptation	CQI and PMI 5ms feedback period
	6ms delay total (measurement in subframe n is used in
	subframe $n + 6$) Quantized CQI, PMI feedback error: 0%
	MCSs based on LTE transport formats
Downlink HARQ	Maximum 3 re-transmissions, IR, no error on ACK/NACK, 8ms delay between re-transmissions
Downlink receiver type	MMSE : based on demodulation reference signal (DM-RS) of the serving cell
Channel estimation	Non-ideal channel estimation on both CSI-RS and DM-RS
Antenna configuration	$(M, N, P) = (8, 4, 2)$
TXRU configuration ($N_H \times N_V$)	1×8, 2×8, 4×8, and 8×8 with X-pol (0.5λ, 0.8λ antenna spacing for vertical and horizontal)
Control channel overhead, Acknowledgments etc.	Control channel: 3 symbols in a
	subframe Overhead of DM-RS: 12
	RE/RB/Subframe
	Overhead of CSI-RS: in maximum 16 REs of CSI-RS every
	5ms per RB (This is, in 8 Tx antenna case, 8 REs/RB per 10ms)
	Overhead of CRS: 2-ports CRS
Channel model	3D urban macro and micro channel model [5] with 3km/h UE speed
Inter-cell interference modeling	57 intercell interference links are explicitly considered.
Max. number of layers	4
Traffic model	Full buffer and non-full buffer (FTP Model) with 0.5 MBytes packet and various arrival rate

REFERENCES

[1]   T. L. Marzetta, "Non cooperative cellular wireless with unlimited numbers of base station antennas", IEEE Trans. Wireless Commun., vol. 9, no. 11, pp.3590 -3600, 2010

[2]   Y. Kim, H. Ji, J. Lee, Y.H. Nam, B.L. Ng, I. Tzanidis, Y. Li and J. Zhang, "Full Dimension MIMO (FD-MIMO): The Next Evolution of MIMO in LTE Systems," Wireless Commun. Mag., vol. 21, issue 3, 2014

[3]   Y. H. Nam, B. L. Ng, Y. Sayana, Y. Li, J. Zhang, Y. Kim and J. Lee, "Full-dimension MIMO (FD-MIMO) for next generation cellular technology," IEEE Commun. Mag., vol. 51, issue 6, 2014

[4]   W. Zhang, J. Xiang, Y.R. Li, Y. Wang, Y. Chen, P. Geng and Z. Lu, "Field Trial and Future Enhancements for TDD Massive MIMO Networks," in Proc. on 26th Intl. Symp. on Personal, Indoor, and Mobile Radio Comm. (PIMRC) Workshop Advancements in Massive MIMO, 2015, pp. 1114-1118

[5]   3GPP Technical Reports TR36.873, "Study on 3D channel model for LTE".

[6]   C. Lim, T. Yoo, B. Clerckx, , B. Lee and B. Shim, "Recent trends in MU-MIMO,", IEEE Commun. Mag., vol. 51, issue 3, 2014.

[7]   N. Jindal, "MIMO broadcast channels with finite-rate feedback." IEEE Trans. on Inform. Theory, vol. 52, issue 11, 2006.

[8]   3GPP Technical Reports TR36.897, "Study on Elevation Beamforming/Full-Dimension (FD) MIMO for LTE".

[9]   3GPP Technical Reports TR36.847, "E-UTRA and UTRA; Radio Frequency (RF) requirement background for Active Antenna System (AAS) Base Station (BS)".

[10]   D. Tse, and P. Viswanath, Wireless Communication. Cambridge University Press, 2005.

[11]   B. Lee, J. Choi, J. Seol, D. Love, and B. Shim, "Antenna grouping based feedback compression for FDD-based massive MIMO systems", IEEE Trans. on Commun., vol. 63, no. 9, pp. 3261-3274, Sept. 2015.

[12]   J. Choi, B. Shim, Y. Ding, B. Rao, and D. Kim, "Compressive sensing for wireless communications: useful tips and tricks", submitted to IEEE Commun. Survey and Tutorials.